

KEK-TH-534
hep-ph/9708376
August 1997

Baryogenesis at the Electroweak Scale and Above *

Hajime AOKI[†]

*Theory Group, KEK,
Tsukuba, Ibaraki 305, Japan*

Abstract

We consider origins of the baryon asymmetry which we observe today. We review the progress of electroweak-scale baryogenesis, and show a new mechanism, string-scale baryogenesis.

*To appear in the Proceeding of the KEK meeting on “*CP* violation and its origin”.

[†] e-mail address : haoki@theory.kek.jp, JSPS research fellow.

1 Introduction

Baryogenesis [1] is one of the important problems in particle physics and cosmology: Why do we live in a universe where there is dominance of matter over anti-matter? How do we explain the observed value of the ratio $n_B/s \sim 10^{-10}$, where n_B is the difference between the number density of baryons and that of anti-baryons, and s is the entropy density? Until now, many baryogenesis scenarios have been proposed, where a nonzero n_B is dynamically generated from a baryon-symmetric initial state within the context of standard hot big bang cosmology.

In the theory of electroweak interactions (the Weinberg-Salam theory), baryon number conservation is violated *via* sphaleron processes due to chiral anomaly. Baryogenesis scenarios at the electroweak scale have been studied recently [2, 3, 4]. They are attractive since they can be tested at the current and near-future terrestrial experiments. Within the minimal standard model (MSM), it is difficult to generate the observed baryon asymmetry, due to the too small CP violation source and the insufficient electroweak phase transition. Some extensions of the MSM resolve these problems and allow generation of the observed baryon asymmetry. We can rule out some models such as the MSM and give constraints to parameter spaces for other models, by requiring successful baryogenesis and including other experimental results. However, many extended models can explain the observed baryon asymmetry, and we cannot specify the model beyond the MSM by these studies now.

Grand unified theories (GUTs), which unify the strong and electroweak interactions, predict baryon number violation at the tree level. The first baryogenesis scenario was proposed in the context of the GUT [5]. There, decays of heavy bosons cause departure from thermal equilibrium. These scenarios can explain the observed baryon asymmetry, although there remain some problems such as super-heavy monopoles which overclose the universe, and the washing out of the generated asymmetry by the sphaleron processes.

String theory is a promising candidate for the unified theory including gravity. It has no symmetry assuring the baryon number conservation, thus the baryon number is thought to be violated at the string scale or the Planck scale. We pointed out a possibility of baryogenesis at the string scale [6]. Even if the MSM describes the nature well above the electroweak scale, it should be modified at the string scale or the Planck scale due to the gravitational effects. Hence it is important to consider these scenarios.

Many other interesting mechanisms have been proposed. In the supersymmetric exten-

sions of the MSM, superpartners of the quarks and leptons are introduced and these scalars could have nonvanishing vacuum expectation values along the flat directions. They oscillate afterwards, which generates baryon asymmetry [7]. Topological defects such as cosmic strings and domain walls, could affect the generation of the baryon asymmetry [8].

In this article, we mainly consider two baryogenesis scenarios: the electroweak baryogenesis and the string-scale baryogenesis. Readers who are interested in the GUT-scale baryogenesis should consult Ref. [1], for example.

In section 2 we review the observational evidence for the existence of a baryon asymmetry of the universe, and three necessary conditions to generate a baryon asymmetry dynamically. In section 3 we review the electroweak baryogenesis, and in section 4 we present the string-scale baryogenesis. The last section is devoted to conclusions and discussions.

2 Baryon Asymmetric Universe

2.1 Evidence for a Baryon Asymmetry of the Universe

Within the solar system we do not observe any bodies of antimatter. High energy cosmic rays are generally believed to be of extra solar origin. The small ratio of antimatter to matter in the cosmic rays, which is consistent as secondary products, is an evidence for baryon asymmetry in our galaxy. The existence of both matter and antimatter galaxies in a cluster of galaxy would lead to a significant γ ray flux from nucleon antinucleon annihilation. The observed γ ray flux suggests that clusters like Virgo cluster must not contain both matter and antimatter galaxies. Therefore we can say that there is matter dominance over antimatter on scales at least as large as $(1 - 100)M_{\text{galaxy}} \approx 10^{12} - 10^{14} M_{\odot}$ ³.

We usually characterize the baryon asymmetry by the ratio, $n_B/s \equiv (n_b - n_{\bar{b}})/s$, where n_b is the number density for baryons, $n_{\bar{b}}$ is that of anti-baryons, and s is the entropy density. This ratio remains constant even in the expanding universe, when there are no baryon number violating processes and no entropy productions. The most stringent constraint on this ratio comes from the big bang nucleosynthesis. The observed primordial abundances for light elements, D, ³He, ⁴He, and ⁷Li, give $\eta \equiv n_B/n_{\gamma} = (1.5 - 6.3) \times 10^{-10}$ [10]. $n_{\gamma} = 2\zeta(3)/\pi^2 T^3 \approx 400\text{cm}^{-3}(T/2.7\text{K})^3$ is the photon number density. Since $s = 2\pi^2/45g_* T^3 \approx 7.04n_{\gamma}$ at

³ It is reported that the domain of matter dominance should be as large as the entire visible universe (a few Gpc), in order that the cosmic diffuse γ -ray spectrum near 1 MeV may not exceed the observational limits [9].

present,

$$n_B/s = (0.21 - 0.90) \times 10^{-10}. \quad (2.1)$$

This is what we usually refer to as the baryon asymmetry of the universe.

2.2 The Tragedy of a Symmetric Cosmology

One might think that the whole universe is baryon symmetric but there are baryon-antibaryon fluctuations in space and we live in a body of matter. However, as we show below, there is no plausible mechanism to separate matter from antimatter on such large scales as galaxy scales.

Statistical Fluctuations: Although the matter-antimatter asymmetry appears to be large today in the sense $(n_b - n_{\bar{b}})/n_b \sim 1$, the fact that n_B/s is small implies that at very early times the asymmetry was small. When the temperature of the universe was higher than 1 GeV, baryons and antibaryons should have been about as abundant as photons, $n_b \approx n_{\bar{b}} \approx n_\gamma$. Since n_B/s is a conserved quantity and the entropy density is $s \approx g_* n_\gamma \approx 10^2 n_\gamma$ at $T \gtrsim 1$ GeV,

$$(n_b - n_{\bar{b}})/n_b \approx (n_b - n_{\bar{b}})/n_\gamma \approx g_* n_B/s \sim 10^{-8} (T \gtrsim 1 \text{ GeV}).$$

This small asymmetry might be explained by the statistical (Poisson) fluctuations. The co-moving volume that encompasses our galaxy today contains about 10^{69} baryons and 10^{79} photons. When $T \gtrsim 1$ GeV it contains about 10^{79} baryons and antibaryons. From statistical fluctuations one can expect the asymmetry, $(n_b - n_{\bar{b}})/n_b \approx 1/\sqrt{n_b V} \sim 10^{-39.5}$, which is too small. Therefore it is impossible to explain the fact that we observe the baryon asymmetry $n_B/s \sim 10^{-10}$ over the galaxy scales, by statistical fluctuations.

Hypothetical Interactions: As the universe cooled down below 1 GeV the number of baryons and antibaryons decreased tracking the equilibrium abundance, as long as annihilation processes were in equilibrium. At $T \sim 20$ MeV the annihilation processes freeze out. The residual ratio of baryon number density to entropy density is about $n_b/s = n_{\bar{b}}/s \sim 10^{-19}$, which is too small. In order to avoid this annihilation catastrophe, suppose that some hypothetical interactions separated matter and antimatter before $T \simeq 38$ MeV when $n_b/s = n_{\bar{b}}/s \sim 10^{-10}$. At that time, however, the causal region (horizon) was small and contained only about $10^{-7} M_\odot$. Hence we cannot explain the asymmetry over the galaxy scales.

2.3 Sakharov's Conditions

Since the baryon symmetric universe is hopeless, we must consider an excess of baryons over antibaryons in the whole universe⁴. Three ingredients are necessary to dynamically generate baryon asymmetry from a baryon-symmetric initial state [11]:

- (1) baryon number nonconservation,
- (2) violation of both C and CP invariance,
- (3) departure from thermal equilibrium.

Without baryon number nonconserving interactions the universe remains baryon-symmetric and baryogenesis cannot occur. Although we have not observed baryon number violating processes in laboratories yet, we believe that there are such interactions. For example, in the electroweak theory baryon number conservation is violated due to chiral anomaly. Grand unified theories also predict baryon number violating processes. Also, at the Planck scale or the string scale baryon number is thought to be violated.

Under C (charge conjugation) and CP (charge conjugation combined with parity), the B (baryon number) of a state changes its sign. Thus a state that is either C or CP invariant must have $B = 0$. If the universe begins with equal amounts of matter and antimatter, and without a preferred direction, then its initial state is both C and CP invariant. Unless both C and CP are violated, the universe will remain either C or CP invariant as it evolves, and thus cannot develop a net baryon number even if B is not conserved. Hence, both C and CP violations are necessary. C is maximally violated in the weak interactions. CP violation has been observed in the K -on system. However the fundamental understanding of CP violation is still lacking, and the studies of baryogenesis is expected to shed light on its understanding.

When baryon-number-changing processes are in chemical equilibrium, the chemical potential for the baryon number vanishes. CPT invariance guarantees the mass equality of baryon and antibaryon. Thus the equilibrium distribution for baryons coincides with that for antibaryons, and thus $n_b = n_{\bar{b}}$. Hence, in equilibrium with active baryon-number-changing processes, no baryon asymmetry is generated and any baryon asymmetry generated before is washed out. However, in the context of the standard big bang cosmology, the universe has experienced nonequilibrium many times, when baryon asymmetry can be generated: Phase transitions accompanied by symmetry breakings, freeze outs of some interactions due to the

⁴ One may consider a symmetric universe where baryogenesis and “anti-baryogenesis” occur in different domains. This is possible if we consider spontaneous CP violation and inflation universe, for example.

expansion of the universe, *etc.*.

3 Electroweak Baryogenesis

3.1 Overview

In the standard model of electroweak interactions, the baryon number (and lepton number) are not conserved due to chiral anomaly [12]. The transition rates of these processes are small at zero temperature, but enhanced to the observable order of magnitude at high temperatures (subsection 3.2). This leads to the fact that any pre-generated baryon asymmetries may be washed out by these anomalous processes in thermal equilibrium, which gives constraints on the models, as we see in subsection 3.3.

In subsection 3.4, we see how baryon asymmetry is generated by the anomalous electroweak processes provided that the theory has CP violation and there is departure from thermal equilibrium. The observed value of the baryon asymmetry can be obtained quite easily in these mechanisms.

However, within the minimal standard model (MSM), it is difficult to generate the observed baryon asymmetry, as we see in subsection 3.5. First of all, CP violation coming only from the CKM phase is too small to explain the observed value. Secondly, the electroweak phase transition should be a strong first order phase transition, in order to realize the departure from thermal equilibrium, and to preserve the generated baryon asymmetry. In the MSM, however, these conditions are not satisfied.

In some extensions of the MSM, the above mentioned problems are resolved and the observed baryon asymmetry can be generated at the electroweak scale. The requirements of successful baryogenesis along with some experimental results rule out some models (such as the MSM), and constrain the allowed parameter regions for other models. In subsection 3.6, we see some extensions of the MSM and their viabilities.

3.2 Baryon Number Violation in the Electroweak Theory

3.2.1 Anomaly and Topological Structure of Vacua

In the standard model of electroweak interactions, the baryon number and lepton number are exactly conserved at the classical level. However, due to chiral anomaly, they are not

conserved on the quantum level [12]:

$$\partial_\mu j_B^\mu = \partial_\mu j_L^\mu = N_f \left[\frac{g^2}{16\pi^2} \text{tr}(W^{\mu\nu} \tilde{W}_{\mu\nu}) - \frac{g'^2}{32\pi^2} B^{\mu\nu} \tilde{B}_{\mu\nu} \right], \quad (3.2)$$

where N_f is the number of generations, $W^{\mu\nu}$ and $B^{\mu\nu}$ are the gauge field strength of $SU_L(2)$ and $U_Y(1)$, respectively, g and g' are their gauge couplings, and $\tilde{W}_{\mu\nu} = \frac{1}{2}\epsilon_{\mu\nu\alpha\beta}W^{\alpha\beta}$. Note that the difference $B - L$ is strictly conserved. The right hand side of this equation is a total divergence:

$$\begin{aligned} \frac{g^2}{16\pi^2} \text{tr}(W^{\mu\nu} \tilde{W}_{\mu\nu}) &= \partial_\mu K^\mu, \\ \frac{g'^2}{32\pi^2} B^{\mu\nu} \tilde{B}_{\mu\nu} &= \partial_\mu k^\mu, \end{aligned}$$

where

$$\begin{aligned} K_\mu &= g^2 \epsilon_{\mu\alpha\beta\gamma} \frac{1}{8\pi^2} \text{tr}(W^\alpha \partial^\beta W^\gamma + \frac{2}{3} g W^\alpha W^\beta W^\gamma) \\ &= g^2 \epsilon_{\mu\alpha\beta\gamma} \frac{1}{8\pi^2} \text{tr}(\frac{1}{2} W^{\alpha\beta} W^\gamma - \frac{1}{3} g W^\alpha W^\beta W^\gamma), \end{aligned} \quad (3.3)$$

$$k^\mu = g'^2 \epsilon_{\mu\alpha\beta\gamma} \frac{1}{32\pi^2} B^{\alpha\beta} B^\gamma. \quad (3.4)$$

Thus, integrating the anomaly equation (3.2), we obtain

$$\Delta B = \Delta L = N_f \Delta(N_{\text{cs}} - n_{\text{cs}}), \quad (3.5)$$

where N_{cs} and n_{cs} are Chern-Simons number,

$$\begin{aligned} N_{\text{cs}} &= g^2 \frac{1}{8\pi^2} \int d^3x \epsilon_{ijk} \text{tr}(W^i \partial^j W^k + \frac{2}{3} g W^i W^j W^k) \\ &= \frac{1}{8\pi^2} \int d^3x \epsilon_{ijk} \text{tr}(\frac{1}{2} G^{ij} W^k - \frac{1}{3} g W^i W^j W^k), \end{aligned} \quad (3.6)$$

$$n_{\text{cs}} = g'^2 \frac{1}{32\pi^2} \int d^3x \epsilon_{ijk} B^{ij} B^k. \quad (3.7)$$

Next, let us consider the vacuum configurations of the gauge field. The Chern-Simons number for $U_Y(1)$, n_{cs} , is strictly zero since the value of the field strength, B^{ij} , takes zero in this case. However, in the non-Abelian gauge theory, the vacuum configuration is a pure gauge, $W_\mu = g^{-1} U \partial_\mu U^\dagger$, and the Chern-Simons number becomes

$$\begin{aligned} N_{\text{cs}} &= -\frac{1}{24\pi^2} \int d^3x \epsilon_{ijk} \text{tr}(U \partial^i U^\dagger U \partial^j U^\dagger U \partial^k U^\dagger) \\ &\equiv \omega(U), \end{aligned} \quad (3.8)$$

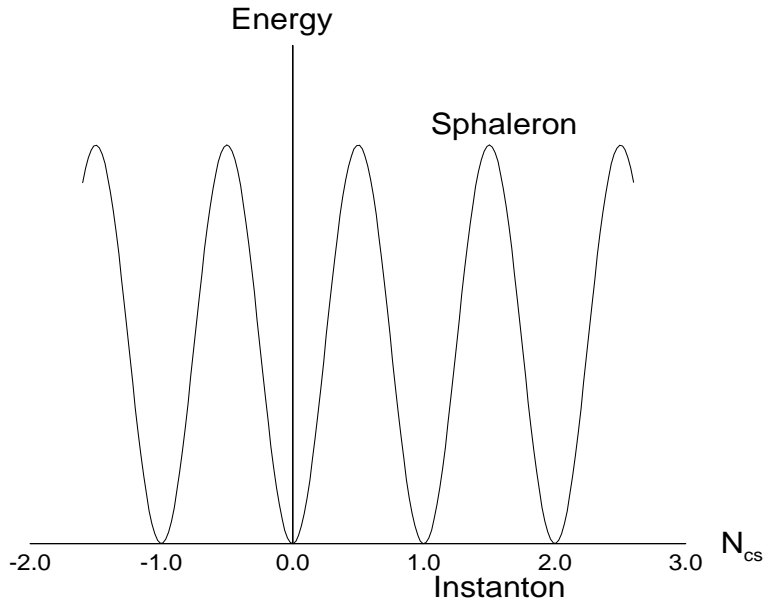


Figure 1: The structure of vacua of non-Abelian gauge theory. There are an infinite number of degenerate vacua labeled by the Chern-Simons number. The sphaleron solution stays at the top of the potential barrier, and the instanton solution is used in analyzing quantum tunneling.

where $\omega(U)$ is a topologically invariant quantity of $\Pi_3(G) \simeq Z$ when we identify spatial infinities. This shows that there are an infinite number of degenerate vacua which are classified by the Chern-Simons number. They cannot be transformed continuously one another within the vacuum configurations. However, for a general configuration other than vacua, the Chern-Simons number takes a fractional value and we can transform continuously one vacuum into another *via* general configurations. Fig. 1 shows the vacuum structure of the non-Abelian gauge theory.

When a transition from one vacuum to a topologically distinct vacuum occurs, baryon number is changed, as you can see from Eq. (3.5). In the next subsections, we consider the rate for baryon number violating processes by estimating the transition rate from one vacuum to another.

In the gauge-Higgs system with nonzero vacuum expectation value of the Higgs field, there exists a saddle-point solution at the top of the barrier between the neighboring vacua in Fig. 1. Such a solution is called “sphaleron” solution [13]. It is an unstable solution and is easy to decay to the vacua. This solution was constructed by considering a noncontractable loop in the configuration space. In the minimal standard model, the energy of the sphaleron solution depends on the ratio of the parameters λ/g and varies between 7.9 TeV for $\lambda = 0$

and 13.7 TeV for $\lambda = \infty$, where λ is the Higgs self coupling constant.

$$E_{\text{sp}} \simeq M_W/\alpha_W \simeq 10 \text{ TeV}. \quad (3.9)$$

The fact that the barrier height is finite suggests that the transition between vacua is likely to occur when the energy or the temperature of the system becomes large [14, 2].

3.2.2 Transition Rate at Zero Temperature

Since the height of the potential barrier is finite, $E_{\text{sp}} \sim 10 \text{ TeV}$, it might be possible that we observe baryon number violating processes in future collider experiments. Let us consider the processes

$$q + q \rightarrow 7\bar{q} + 3\bar{l} + n_W W + n_H H, \quad (3.10)$$

where n_W and n_H are the numbers of the produced gauge bosons and Higgs bosons, respectively, and they take arbitrary numbers. The cross sections for these processes can be obtained by calculating the Green functions semi-classically about instanton-like configurations. Instanton is a classical solution of Yang-Mills theory in four-dimensional Euclidean space-time, which connects the topologically distinct vacua [15]. We will see below that the modification of the instanton solution is useful to estimate the anomalous cross sections in high energies.

The cross sections for vacuum-to-vacuum transitions are exponentially suppressed by the factor of e^{-2S_I} where S_I is the instanton action [12]. These processes had been therefore considered as hopelessly unobservable. However, Ringwald [16] and Espinosa [17] showed that the cross section grows to an observable order of magnitude at high energies $\sim E_{\text{sp}}$ when $O(1/\alpha)$ number of gauge and Higgs bosons are involved in the final state⁵. Unfortunately, their results break the unitarity bound in these energies, suggesting that their leading-order estimations are too naive and higher-order corrections must be considered at least in these energies. Since then, a lot of modifications to their calculations have been made (for reviews see Ref.[20, 4]). Among them, the techniques of calculating the quantum corrections for the final states are developed. Khoze and Ringwald showed an optimistic result suggesting that the anomalous cross section reaches an observable order without breaking the unitarity bound at the energies of the order of E_{sp} ($\sim 10\text{TeV}$), by ‘‘valley method’’ [21]. In this method, the

⁵ Since there is no instanton solution as an exact classical solution in the $SU(2)$ gauge-Higgs system, they used the so-called constraint instanton configurations [18]. It is reported that calculations with valley instantons gives the similar result [19].

total cross section in the instanton background is computed *via* optical theorem, by taking the imaginary part of the forward elastic scattering amplitude in the instanton-anti-instanton background, so that the final state corrections are automatically included.

However, by considering the fermions in the intermediate states, we can see that the cross sections for baryon number violating processes cannot grow so rapidly at high energies as their result [22, 23]. Since we are interested in the “anomalous” cross sections, we have to extract the correct part from the forward elastic scattering amplitude, *i.e.*, the part where the fermion number in the intermediate state is topologically correct in the background of instanton-anti-instanton configuration, and not just the same as that of the initial (and final) state. It is known that when the incident energy is increased, the dominant configurations are the ones where the separation between instanton and anti-instanton is much smaller than the instanton size [21]. Since such configurations seem to be non-anomalous, the anomalous part may be only a tiny fraction of the optimistic estimate of the cross section.

Another severe suppression comes from the initial state corrections, while in the valley method only the final state corrections are considered. This can be understood intuitively as follows: since the sphaleron solution has the spacial extension of the order of M_W^{-1} [13], it is difficult to create such a configuration from the initial state of high energies $\sim E_{\text{sp}}$. On the other hand, when the initial state consists of a large number ($O(1/\alpha_W)$) of particles whose energies are about M_W , as in the case of high temperature systems, the transition can occur at unsuppressed rate. Indeed, the formulations were proposed, where the S-matrix element and the cross section are calculated by functional integrations [24, 25]. The dominant classical configurations are given by solving the equation of motion with correct boundary conditions imposed by the initial and final states. In the case where many particles are involved in both initial and final states, the solutions exist and the cross sections are enhanced in high energies. However, when the initial state involves a few particles, solutions have not been discovered yet, suggesting that the transitions will be suppressed even in high energies (for review, see [4]).

3.2.3 Transition Rate at Non-Zero Temperature

As discussed in the previous subsections, the transition rate of the anomalous processes is expected to be enhanced at high temperatures.

Langer [26] and Affleck [18] developed a technique for evaluating the transition rate of a system over a barrier at finite temperature. They reduce the theory to one dimension,

compute the flux of the system across the barrier in this direction weighted with a Boltzmann factor for each possible initial state, and finally reintroduces the degrees of freedom transverse to this one mode. The formula for the transition rate is

$$\Gamma \simeq \frac{\omega_-}{\pi T} \text{Im}F, \quad (3.11)$$

where F is the free energy of the system evaluated about the configuration at the top of the potential barrier (the sphaleron solution), and ω_- is the negative mode frequency for this configuration. Note that the sphaleron solution is unstable and has the negative mode, which gives the imaginary part of the free energy. The transition rate per unit volume was estimated in the $SU(2)$ gauge-Higgs system [28, 29]:

$$\Gamma_{\text{sp}} = \gamma(\alpha_W T)^{-3} M_W^7 e^{-E_{\text{sp}}/T} \quad (\text{broken phase}), \quad (3.12)$$

where the constant γ involves the Gaussian integrations for the sphaleron solution, and was estimated numerically in Ref. [29]. We refer to this rate as the ‘‘sphaleron transition rate’’. This rate is strongly suppressed by the Boltzmann factor up to temperatures of hundreds of GeV.

In the symmetric phase where the Higgs field has a vanishing vacuum expectation value, the above results are no longer valid. We could find a path which connects topologically distinct vacua in the configuration space, with arbitrary small potential energy at each point. Although there is no reliable theory to estimate the transition rate, a simple dimensional argument allows us to estimate it: In order to generate an $O(1)$ change in baryon number (and Chern-Simons number), the anomaly equation (3.2) implies that a gauge field of spatial extent R must have a field strength of order $(gR^2)^{-1}$. The energy of these configurations are of the order of $(g^2R)^{-1}$. Thus, the smallest value of R for which thermal transitions through such configurations are not strongly suppressed by the Boltzmann factor is $R \sim (g^2T)^{-1}$. This in fact is the dominant spatial scale, since the entropy favors the smaller configurations. From dimensional arguments, the transition rate per unit volume will be proportional to R^{-4} , and thus the result is⁶

$$\Gamma_{\text{sp}} = \kappa(\alpha_W T)^4 \quad (\text{symmetric phase}). \quad (3.13)$$

Although there is no sphaleron solution in the symmetric phase, we call ‘‘sphaleron transition rate’’ in this case, too. The formula (3.13) was checked numerically, and the coefficient κ was

⁶ There is an argument that damping effects in the plasma suppress the sphaleron transition rate by an extra factor of α_W [31].

given to be of order one [30]. The procedure is first generating an ensemble of configurations according to the Boltzmann weight, then considering the time evolution of each configuration by solving the equation of motion, calculating the Chern-Simons number for it, and finally taking the ensemble average over the initial configurations. The result $\langle N_{cs}(t)^2 \rangle_T$ can be fitted to the expression for the random walk ΓVt , and the transition rate Γ is obtained.

3.3 Survival of Primordial Baryon Asymmetry

Before going into the stories of how baryon asymmetry is generated by the sphaleron processes, we consider how the primordial baryon asymmetry is (or is not) washed out by them. Once the sphaleron transition is in equilibrium, any primordial baryon asymmetry is washed out, as mentioned in subsection 2.3. The sphaleron transition rate (3.12), (3.13) exceeds the expansion rate of the universe ($\sim g_*^{1/2} T^2/m_{\text{pl}}$), where m_{pl} is the Planck mass and g_* is the number of relativistic species, in the following region of temperatures:

$$\begin{aligned} T_{\min} &< T < T_{\max}, \\ T_{\min} &\sim T_c \sim 100 \text{ GeV}, \\ T_{\max} &\simeq \alpha_W^4 m_{\text{pl}}/g_*^{1/2} \simeq 10^{12} \text{ GeV}, \end{aligned} \tag{3.14}$$

where T_c is the critical temperature of the electroweak phase transition.

First, let us consider the case where baryon asymmetry was produced at temperature $T > T_{\max}$, for example, the GUT scale or the string scale. Since $B - L$ is conserved in the sphaleron processes, one might think that $B + L$ is washed out and survival baryon and lepton asymmetries are $B = -L = \frac{1}{2}(B - L)_{\text{initial}}$, where subscript ‘‘initial’’ refers to the primordial asymmetry [2]. In fact, the situation is more complicated: The sphaleron processes only involve the left-handed fermions, and the charge neutrality of the universe must be preserved. Thermodynamical calculations lead to the results

$$\begin{aligned} B &= \frac{8N_f + 4m}{22N_f + 13m} (B - L)_{\text{initial}}, \\ L &= -\frac{14N_f + 9m}{22N_f + 13m} (B - L)_{\text{initial}} \quad (\text{symmetric phase}), \end{aligned} \tag{3.15}$$

for the case in the symmetric phase, and

$$\begin{aligned} B &= \frac{8N_f + 5(m + 2)}{24N_f + 13(m + 2)} (B - L)_{\text{initial}}, \\ L &= -\frac{16N_f + 9(m + 2)}{24N_f + 13(m + 2)} (B - L)_{\text{initial}} \quad (\text{broken phase}), \end{aligned} \tag{3.16}$$

for the broken phase, where N_f and m are the number of generations and Higgs bosons, respectively [33]. Anyway, if the primordial baryon asymmetry is generated by the $(B - L)$ conserving processes (which is the case in the minimal $SU(5)$ GUT model [34]), it is completely washed out.

Next, let us consider the case where there are some new interactions, which violate lepton number or baryon number, and are in thermal equilibrium for some period between T_{\min} and T_{\max} . Combining them with the anomalous electroweak interactions, both baryon and lepton asymmetries are washed out. In order to avoid this problem, the new interactions must freeze out above the temperature T_{\max} . For example, let us consider a lepton number violating interaction

$$\mathcal{L} = \frac{m_\nu}{v^2} ll\phi\phi, \quad (3.17)$$

where m_ν is the neutrino mass, v is the vacuum expectation value of the Higgs field, and l and ϕ are the lepton and Higgs doublets, respectively. The above mentioned condition for the survival of the primordial baryon asymmetry gives an upper bound on the neutrino mass [32, 33]⁷:

$$m_\nu \lesssim g_*^{1/2} v^2 / m_{\text{pl}} \alpha_w^2 \sim 10^{-1} \text{ eV}. \quad (3.18)$$

Finally, let us consider the case where a baryon asymmetry is generated by the sphaleron processes at the first order electroweak phase transition. Even if a baryon asymmetry is generated, it is washed out in the broken phase (true vacuum) just after generated, if the sphaleron transition processes in the broken phase are in equilibrium. The sphaleron transition rate in the broken phase at the electroweak phase transition, depends sensitively on the sphaleron energy (see Eq. (3.12)), which will be proportional to the vacuum expectation value of the Higgs field. Thus the condition for the survival of the generated baryon asymmetry is [36]

$$v(T_c)/T_c \gtrsim 1, \quad (3.19)$$

where $v(T_c)$ is the vacuum expectation value of the Higgs field in the broken phase at the critical temperature, T_c .

⁷ In fact, since the Yukawa coupling is small, the right-handed lepton number is effectively conserved. Thus this constraint is weakened [35].

3.4 Mechanisms of Electroweak Baryogenesis

Since the baryon number violating processes occur rapidly at high temperatures, a baryon asymmetry is generated if there is a bias to prefer the direction of increasing baryon number. From detailed balance, we obtain the equation

$$\frac{dn_B}{dt} = -N_f^2 \frac{\mu_B \Gamma_{\text{sp}}}{T}, \quad (3.20)$$

where N_f is the number of flavors, Γ_{sp} is the sphaleron transition rate (3.12) (3.13), and μ_B is the chemical potential for baryon number⁸. The factor N_f^2 arises since N_f baryon number is changed in one sphaleron transition. From dimensional analysis, we can expect that the baryon-to-entropy ratio of the order of

$$\frac{n_B}{s} \sim N_f^2 \frac{\kappa \alpha_W^4}{g_*} \sim 10^{-7} \quad (3.21)$$

will be generated, provided that there is enough nonequilibrium distributions of matter, and the theory has enough CP violation.

As we will see below, if the electroweak phase transition is first order, nonequilibrium distribution is realized around the bubble wall. If we consider the two-Higgs-doublet model, for example, there is enough CP violating phase in the Higgs potential. The vacuum expectation values of the Higgs fields take complex values in general, and their relative phase cannot be reduced to zero by field redefinition. The bubble wall at the phase transition will have a profile like

$$\phi(z) = v \left[\frac{1 - \tanh(z/l_w)}{2} \right] e^{-i\Delta\theta[1+\tanh(z/l_w)]/2}, \quad (3.22)$$

where z is the coordinate perpendicular to the wall, l_w is the wall width, and $\Delta\theta$ is the difference of the complex phases between in the symmetric phase and in the broken phase. Through the Yukawa couplings, fermions interact with this CP violating bubble wall, which can cause nonzero chemical potential for baryon number.

Let us consider characteristic time scales governing the relevant reactions: The time scale for the universe expansion, τ_H , the sphaleron transition, τ_{sp} , the thermalization processes due to strong and weak interactions, τ_{th} , and the time scale to cause nonequilibrium distributions, measured by how fast the wall passes through a point in the plasma, τ_{wall} . At the electroweak

⁸ Another form of this equation is written in Ref. [37]: $\frac{dn_B}{dt} = -N_f n_{f_L} \frac{\Gamma_{\text{sp}}}{T^3/6}$, where n_{f_L} is the number density of left-handed fermions.

phase transition, they are estimated to be [40]

$$\begin{aligned}
\tau_H^{-1} &\simeq 1.66 g_*^{1/2} \frac{T^2}{m_{\text{pl}}} \sim 10^{-16} T, \\
\tau_{\text{sp}}^{-1} &\simeq \alpha_W^4 T \sim 10^{-6} T, \\
\tau_{\text{th}}^{-1} &\sim \begin{cases} 0.25 T & \text{for quarks} \\ 0.08 T & \text{for leptons,} \end{cases} \\
\tau_{\text{wall}}^{-1} &\simeq \frac{v_w}{l_w} \sim (0.01 - 1) T,
\end{aligned} \tag{3.23}$$

where v_w is the velocity of the wall. Since $\tau_H^{-1} \ll \tau_{\text{sp}}^{-1} \ll \tau_{\text{wall}}^{-1}$, the sphaleron transitions cannot be out of equilibrium by the expansion of the universe, but they can be out of equilibrium in the first order electroweak phase transition.

Let us consider the following two extreme cases:

- 1) $\tau_{\text{th}}^{-1} \ll \tau_{\text{wall}}^{-1}$, thin wall case. In this case, the fermions interact with the bubble wall like quantum mechanical particles, reflected and transmitted by a potential barrier, and their interactions with the particles in the plasma are neglected, when they propagate across the wall.
- 2) $\tau_{\text{th}}^{-1} \gg \tau_{\text{wall}}^{-1}$, thick wall case. In this case, the fermions are scattered by the particles in the plasma, which can be described by the thermodynamics in equilibrium, and the quantum reflection by the wall can be neglected.

Mechanisms for baryogenesis were proposed [38, 39] in these two cases. In both cases, the expected value (3.21) is obtained with the optimal parameters for $\Delta\theta$, l_w , *etc.*, thus the observed baryon asymmetry can be explained in quite large regions of parameter space.

3.4.1 The Thin Wall Case: Charge Transport Mechanism

Since the bubble wall has a CP violating complex phase (3.22), when the fermions are scattered off the wall, a net charge is reflected from the wall, which is transported into the region preceding the bubble. This charge asymmetry can bias the sphaleron transitions in the symmetric phase and generate a baryon asymmetry. [3, 39]

The procedure to calculate the baryon asymmetry in this mechanism is as follows:

- 0) Compute the wall profile and velocity, including the space dependent CP violating phase, from the finite temperature effective potential (or effective action). The form of CP violating bubble wall is studied [41], although in Ref. [39], the wall profile is assumed to be (3.22).
- 1) Calculate the reflection coefficients for fermions striking the wall, by integrating the Dirac (or Majorana) equation of motion in the wall-rest frame. Because of CP violation, the

reflection coefficient for particles and antiparticles can be different.

$$\Delta R \equiv R_{R \rightarrow L} - R_{\bar{R} \rightarrow \bar{L}} \neq 0 \quad (3.24)$$

2) Convolute the reflection coefficients with the incoming (boosted) flux of particles in the plasma, to determine the outgoing flux from the wall into the symmetric phase. Due to the nonzero difference between the reflection coefficients for particles and antiparticles, this flux carries nonzero quantum numbers X ; for example, chiral charge. In Ref. [39], they consider the hypercharge since it is conserved in the symmetric phase.

3) The nonzero flux from the wall, F_X leads to a nonzero charge density distribution, $n_X(z)$ in the region preceding the wall. One can calculate how far the charge is transported into the symmetric phase, by Monte Carlo simulation or solving the Boltzmann equation.

4) The nonzero charge density causes a nonzero chemical potential for baryon number:

$$\mu_B = C \frac{n_X}{T^2}, \quad (3.25)$$

where C is a constant of the order one, and is given by thermodynamical calculations.

5) One can calculate the baryon number density, by integrating the equation (3.20)

$$\begin{aligned} n_B &= - \int dt N_f^2 \frac{\mu_B \Gamma_{\text{sp}}}{T} \\ &\simeq -C N_f^2 \frac{\kappa \alpha_W^4 T}{v_w} \int_0^\infty dz n_X(z), \end{aligned} \quad (3.26)$$

where we assume that the sphaleron transition rate in the broken phase is negligible. Thus, in the above equation, the charge density is integrated from the wall to the symmetric phase. While the bubble wall sweeps the whole universe, the nonzero baryon number density is generated in any point of the space.

The baryon-to-entropy ratio is

$$\frac{n_B}{s} \simeq -C N_f^2 \frac{\kappa \alpha_W^4}{g_*} \frac{F_X}{v_w T^3} \tau T, \quad (3.27)$$

where τ is the transport time within which the scattered fermions are transported into the symmetric phase and captured by the wall. The result of Monte Carlo simulation shows $\tau T \sim 10 - 10^3$ for the top quark [39], rather large value compared with its diffusion constant $D \sim T^{-1}$. It is because particles are scattered primarily in forward direction. The baryon-to-entropy ratio reaches 10^{-7} , when the top quark scattering is considered, the CP violation parameter $\Delta\theta$ is taken to be of the order one, and the wall width is assumed to be of the order T^{-1} [39, 42].

3.4.2 The Thick Wall Case: Spontaneous Baryogenesis

In the thick wall case, one can treat the plasma around the bubble wall as being in quasi-equilibrium, with a classical time-dependent field. However, some reactions such as baryon number violating processes are not in chemical equilibrium, since $\tau_{\text{sp}}^{-1} \ll \tau_{\text{wall}}^{-1}$. Thus the CP violating complex phase in the bubble wall (3.22) may give nonzero chemical potential for baryon number. [3, 38]

To see this, redefine the fermion fields by phase factor, to remove the phase from the Yukawa interaction. This leads to a new interaction from the fermion kinetic energy term:

$$\mathcal{L}_{\text{K.E.}} \rightarrow \mathcal{L}_{\text{K.E.}} + \partial_\mu \theta j^\mu, \quad (3.28)$$

where j^μ is the current associated with the fermion-field redefinition. From the time component of this new interaction, we can see that $\dot{\theta}$ corresponds to the chemical potential for the charge associated with the current j^μ . In Ref. [38], they redefine the fermion fields according to their hypercharge, since the hypercharge is anomaly free so that generation of new interaction $\theta F \tilde{F}$ is avoided.

This nonzero ‘‘chemical potential’’ $\dot{\theta}$ causes a nonzero chemical potential for baryon number:

$$\mu_B = C' \dot{\theta}, \quad (3.29)$$

where C' is a constant of order one, and is given by thermodynamical calculations. This bias generate a nonzero baryon number density, which is calculated by integrating the Eq. (3.20):

$$\begin{aligned} n_B &= - \int dt N_f^2 \frac{\mu_B \Gamma_{\text{sp}}}{T} \\ &\simeq -C' N_f^2 \kappa \alpha_W^4 T^3 (\Delta\theta)_{\text{co}}. \end{aligned} \quad (3.30)$$

Here, we assume that the sphaleron transition rate goes rapidly to zero as the vacuum expectation value of the Higgs field approaches a value $\phi_{\text{co}} e^{i\theta_{\text{co}}}$ in the bubble wall. $(\Delta\theta)_{\text{co}}$ is the difference between θ_{co} and the value of θ in the symmetric phase. Thus, the baryon-to-entropy ratio is

$$\frac{n_B}{s} \simeq -C' N_f^2 \frac{\kappa \alpha_W^4}{g_*} (\Delta\theta)_{\text{co}}. \quad (3.31)$$

It was pointed out that when ϕ_{co} takes a small value, another small factor decreases the result (3.31) and this scenario cannot generate enough amount of baryon asymmetry [43]. In the symmetric phase, where the vacuum expectation value of the Higgs field vanishes, its complex phase θ has no physical meaning, and no baryon asymmetry is generated by this

mechanism. Accordingly, when the vev is small, there must be some suppression factor to the result (3.31).

Until now we consider the case where a baryon asymmetry is generated only in a small region within the bubble wall: $z_{\text{co}} < z < z_{\text{sym}}$, where z_{co} is the position in the wall where the sphaleron transition rate is cutoff, and z_{sym} is the surface between the wall and the symmetric phase. However, if we consider the effect of diffusion, nonzero charges are diffused from within the bubble wall, and a baryon asymmetry can be generated in a wide region in the symmetric phase [44, 37]. Solving the diffusion equation, one concludes that the resultant baryon-to-entropy ratio is of the order of 10^{-7} , irrespective of the value of z_{co} , the profile of the wall, and wall velocity. Now it is established that transport of CP violating quantum numbers into the symmetric phase plays an important role in electroweak baryogenesis for all values of bubble wall widths.

3.5 Baryogenesis within the Minimal Standard Model

Within the MSM, it is difficult to generate the observed baryon asymmetry of the universe. First of all, CP violation coming only from the CKM phase is too small to explain the observed value. Secondly, the electroweak phase transition should be a first order phase transition in order to realize the departure from thermal equilibrium, as we saw in subsection 3.4. Moreover, in order to avoid the washing out of the generated baryon asymmetry, the vacuum expectation value of the Higgs field in the broken phase at the critical temperature must be sufficiently large (subsection 3.3). In the MSM, however, these conditions are not satisfied.

3.5.1 CP violation

Within the MSM with three generations, a CP violating complex phase is in the Cabibbo-Kobayashi-Maskawa (CKM) matrix [45]. This phase could be rotated away if any pair of quarks of the same charge were degenerate in mass, or if any of the mixing angles vanished. Thus, any physical observables related to CP violation will be proportional to a basis-invariant combination [46]

$$d_{CP} = \sin(\theta_{12}) \sin(\theta_{23}) \sin(\theta_{31}) \sin(\delta_{CP}) \\ \times (m_t^2 - m_c^2)(m_t^2 - m_u^2)(m_c^2 - m_u^2)(m_b^2 - m_s^2)(m_b^2 - m_d^2)(m_s^2 - m_d^2). \quad (3.32)$$

The natural mass scale in the electroweak baryogenesis seems to be the temperature, $T \sim 100$ GeV. From dimensional arguments, CP violating observables will be suffer from a suppression factor

$$\frac{d_{CP}}{T^{12}} \sim 10^{-18}. \quad (3.33)$$

Hence the baryon-to-entropy ratio will be of the order of

$$\frac{n_B}{s} \sim N_f^2 \frac{\kappa \alpha_W^4}{g_*} \frac{d_{CP}}{T^{12}} \sim 10^{-25}. \quad (3.34)$$

The above arguments would be invalid and the observed baryon-to-entropy ratio could be generated, if the natural scale were not the temperature but, for example, the mass difference between the strange and down quarks. In Ref. [47], they considered the scattering of the quarks off the bubble wall in the plasma, and pointed out that in some energy regions, the s quark is totally reflected but the d quark is partly reflected and partly transmitted, which enables us to avoid GIM cancellation. However, the quasi-particles in the plasma decay rapidly due to the strong interactions, and the resultant baryon asymmetry is not enhanced appreciably, remaining at the value of Eq. (3.34) [48].

3.5.2 Phase Transition

The standard approach to analyzing phase transition is computing the finite temperature effective potential [49]. For high temperatures, the one-loop effective potential is approximated by the high-temperature expansion:

$$V(\phi, T) = D(T^2 - T_0^2) - ET\phi^3 + \frac{\lambda_T}{4}\phi^4, \quad (3.35)$$

where

$$\begin{aligned} D &= \frac{1}{8v_0^2}(2m_W^2 + m_Z^2 + m_t^2), \\ E &= \frac{1}{4\pi v_0^3}(2m_W^3 + m_Z^3) \sim 10^{-2}, \\ T_0^2 &= \frac{1}{4D}(m_H^2 - 8Bv_0^2), \\ B &= \frac{3}{64\pi^2 v_0^4}(2m_W^4 + m_Z^4 - 4m_t^4), \\ \lambda_T &= \lambda - \frac{3}{16\pi^2 v_0^4}(2m_W^4 \ln \frac{m_W^2}{a_B T^2} + m_Z^4 \ln \frac{m_Z^2}{a_B T^2} - 4m_t^4 \ln \frac{m_t^2}{a_F T^2}). \end{aligned} \quad (3.36)$$

Here $v_0 = 246$ GeV is the value of the Higgs field at the minimum of $V(\phi, 0)$, $\lambda = m_H^2/2v_0^2$ is the Higgs self coupling constant, and $\ln a_B = 2 \ln 4\pi - 2\gamma \simeq 3.51$, $\ln a_F = 2 \ln \pi - 2\gamma \simeq 1.14$.

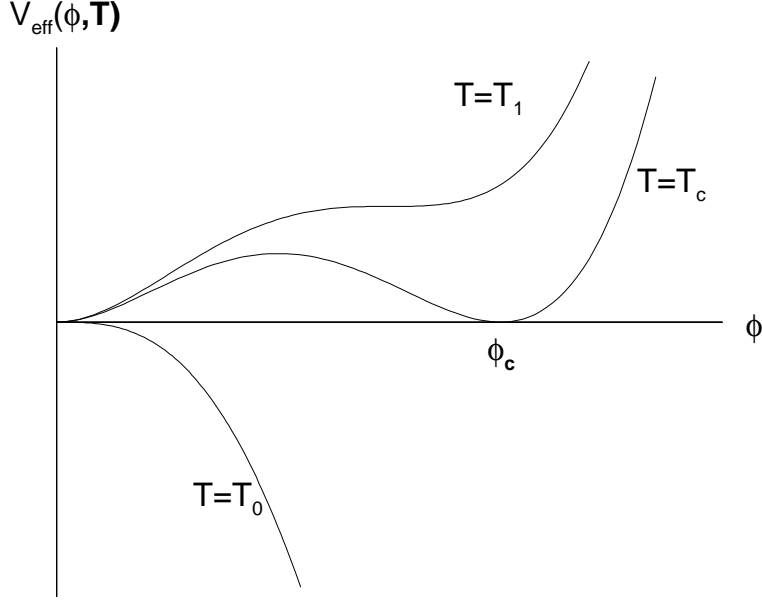


Figure 2: Qualitative form of the effective potential as a function of temperature. It seems to suggest a first order phase transition.

The behavior of the effective potential is depicted in Fig. 2. At very high temperature the only minimum of the potential is at $\phi = 0$. A second minimum appears at $T = T_1$, where,

$$T_1^2 = \frac{T_0^2}{1 - 9E^2/8\lambda_{T_1}D}. \quad (3.37)$$

The value of the field in this minimum at $T = T_1$ is equal to

$$\phi_1 = \frac{3ET}{2\lambda_{T_1}}. \quad (3.38)$$

The values of the potential in the two minima become equal to each other at $T = T_c$, where,

$$T_c^2 = \frac{T_0^2}{1 - E^2/\lambda_{T_c}D}. \quad (3.39)$$

At that moment the field ϕ in the second minimum becomes equal to

$$\phi_c = \frac{2ET_c}{\lambda_{T_c}}. \quad (3.40)$$

The minimum of the potential at $\phi = 0$ disappears at $T = T_0$, when the value of the scalar field in the second minimum becomes equal to $\phi_0 = 3ET_0/\lambda_{T_0}$.

It seems that at some lower temperature than T_c , first-order phase transition occurs. When the Higgs mass is light and λ is small, ϕ_c and the potential barrier between the two minima become large, suggesting the strong first-order phase transition. Indeed, it

was checked that if the Higgs boson mass is smaller than about the masses of W and Z bosons, bubbles of the new phase are nucleated and expand to fill the whole universe [40]. The propagations of the bubble walls make the distribution of particles around the wall in nonequilibrium, which may generate a baryon asymmetry of the universe.

In order to avoid the washing out of the generated baryon asymmetry, the sphaleron transition rate must be small in the broken phase at the phase transition, leading to the condition $\phi_c/T_c \gtrsim 1$ (3.19). Using Eq. (3.40) as a first approximation, this condition gives an upper bound on λ , and thus on the Higgs boson mass [36]:

$$m_H \lesssim 45 \text{ GeV} \quad (3.41)$$

It is already inconsistent with the present experimental lower bound $m_H \gtrsim 70 \text{ GeV}$. Hence, the observed baryon asymmetry cannot be explained within the MSM.

Next, let us consider higher-order corrections to the one-loop effective potential presented above, and a reliability of perturbation expansions. Theories with massless or light particles suffer from the problem of infrared divergences at high temperatures. For example, the longitudinal component of gauge boson is screened in a plasma, and the corresponding Debye mass is $m_{\text{Debye}}^2 = 11/6 g_W^2 T^2$ in one-loop approximation. It becomes larger than the tree level contribution to the W boson mass, $m_W^2 = 1/4 g_W^2 \phi^2$ in the region $\phi/T < O(1)$, suggesting that the naive perturbation expansion is not reliable. This one-loop Debye screening effects can be resummed to all orders in perturbation expansions by substituting $m_W^2 + m_{\text{Debye}}^2$ for m_W^2 in the propagators. This corresponds to the resummation of ring- or daisy-diagrams.

The ring-resummed one-loop calculation indicates that the phase transition becomes weaker than in the naive one-loop calculation, and the upper bound on the Higgs boson mass becomes more severe: $m_H \lesssim 35 \text{ GeV}$ [40]. The ring-resummed two-loop calculation indicates stronger phase transition and relaxes the upper bound: $m_H \lesssim 40 \text{ GeV}$ [50, 51]. In fact, since the top quark is heavy, the phase transition becomes much weaker when its effect is included, and the condition $\phi_c/T_c \gtrsim 1$ cannot be satisfied in any value of the Higgs boson mass.

When the Higgs mass is large, the two-loop-order corrections become huge and the perturbation expansions do not converge even with the ring-resummation. We should say that the perturbative calculations of the effective potential are not reliable in the realistic range of the Higgs boson mass, $m_H \gtrsim 70 \text{ GeV}$, and we should use another method to analyze electroweak phase transition in the MSM.

Lattice simulation is a non-perturbative method for the analysis of the phase transition. Two approaches have been applied for this study. One is to employ the original four-dimensional model [52, 53, 54]. The other is to treat a three-dimensional model derived from the original model by dimensional reduction in time direction [55, 56]. They analyzed the Monte-Carlo time history, the finite-size scaling, the correlation length, the latent heat, the interface tension, *etc.* When the Higgs mass is small, their results reproduce those of the perturbative analysis: the phase transition is of the first order, and the strength of the phase transition becomes weaker as the Higgs boson mass increases. Moreover, they showed that the first-order phase transition terminates at around $m_H \sim 80 \text{ GeV}$, and two phases are connected at larger Higgs masses. Thus, if the Higgs mass is larger than this critical value, no baryon asymmetry can be generated at the electroweak scale.

3.6 Beyond the Minimal Standard Model

In contrast to the MSM, in most extensions of the MSM there can be new CP violation sources other than the CKM phase, which could be an origin of the observed baryon asymmetry. Also, since there are more parameters, the electroweak phase transition can be sufficiently strong first-order to avoid the washing out of the generated baryon asymmetry, in some region of the parameter space. However, other experimental constraints such as electric dipole moments (EDM) of neutron and atoms must be considered to check whether the model is viable.

In the two-Higgs-doublet model, there is a new CP source in the Higgs potential and an enough amount of baryon asymmetry can be generated, as we saw in subsection 3.4. The experimental constraints of EDM allow the CP phase to be as large as $O(1)$ [57]. The experimental lower bound on the mass of the lightest Higgs boson and the requirement of the sufficiently strong first-order phase transition can be simultaneously satisfied in a wide range of the parameter space [58]. Therefore, this model will be viable.

In the minimal supersymmetric standard model (MSSM)⁹, the phase transition can be sufficiently strongly first order only in a restricted region of the parameter space¹⁰ [59, 60]:

$$m_{\tilde{t}_R} \lesssim 175 \text{ GeV}, m_h \lesssim 80 \text{ GeV}, m_A \gtrsim 200 \text{ GeV}, \tan \beta \lesssim 2.5, \tilde{A}_t \simeq 0. \quad (3.42)$$

⁹By MSSM we mean the supersymmetric extension of the standard model with minimal particle content and R parity conservation, whereas the constraint MSSM includes the assumption of coupling constant unification, universal squark and gaugino masses and universal trilinear couplings at the unification scale.

¹⁰ Two-loop calculations show stronger phase transition, thus these bounds will be relaxed [61].

Here $m_{\tilde{t}_R}$ is the mass of the stop (supersymmetric partner of the top quark), m_h is that of the lightest Higgs boson, m_A is that of the pseudoscalar Higgs boson, $\tan\beta$ is the ratio of the vacuum expectation values of the two Higgs bosons, and $\tilde{A}_t = A_t + \mu/\tan\beta$ is the effective $\tilde{t}_L - \tilde{t}_R$ mixing parameter. The upper bound on the lightest Higgs mass, 80 GeV, can be reached by the LEP2 experiments, and the upper bound on the stop mass by the Tevatron.

There can be new CP violating phases in the soft supersymmetry breaking terms in the MSSM. The observed value of the baryon asymmetry can be generated at the electroweak phase transition if the new CP phases are larger than about 10^{-2} [62, 63, 64]. However the presence of these new phases also lead to the neutron EDM. The experimental bound tells us that either these phases are less than about 10^{-2} [65] or the squark masses are very large $m_{\tilde{u}} \gtrsim 1$ TeV [66]. Thus, if the present baryon asymmetry is generated by this mechanism, either neutron EDM will be discovered soon or the first generation squarks are heavy.

Also, large mixings between the right-handed up-type squarks, $\tilde{c}_R - \tilde{t}_R$ or $\tilde{u}_R - \tilde{t}_R$, along with the CP violating phase already present in the quark mass matrix, lead to the generation of the observed baryon asymmetry and the sufficiently strong electroweak phase transition [67]. This scenario predicts $D - \bar{D}$ mixing at a level that should be discovered soon. Thus the possibility of baryogenesis in the MSSM significantly constraints its parameter space, and near future experiments will shed light on this picture.

Other extended models such as a model with heavy neutrinos [68] and a model with vector-like quarks [69, 70], were studied and the observed baryon asymmetry can be generated in certain parameter regions in these models.

4 String-Scale Baryogenesis

4.1 Overview

In this section we consider baryogenesis scenarios at the string scale or the Planck scale, and show how the observed baryon asymmetry can be explained in these new scenarios [6]. Even if the minimal standard model (MSM) describes the nature well above the electroweak scale, it must be modified around the string scale or the Planck scale due to gravitational effects. Hence it is important to consider the baryogenesis scenarios at these scales.

At the string and Planck scales, the Sakharov's three necessary conditions for baryogenesis are satisfied. In string theory, there is no symmetry assuring the baryon number conservation. Also, when we consider string inspired models or effective theories with a

cut-off at the string scale, there is no reason to prohibit baryon- or lepton-number violating interactions in theories with a cut-off. On the other hand, the MSM, which is required to be renormalizable and gauge invariant, does not allow such interactions. Sources of CP violation at the string scale can differ from those at the electroweak scale, and other sources than the CKM phase are allowed at the string scale.

As for departure from thermal equilibrium, we use the so called Hagedorn temperature [71, 72]. String theory has a limiting temperature, where the higher excited states of string theory are occupied. The decay processes of these states will cause nonequilibrium distributions. Baryon asymmetry is generated during the decay of the higher excited states. It is also generated after the decay since nonequilibrium distributions caused by the decay processes are maintained until the rates for thermalization processes dominate the expansion rate of the universe.

The resultant baryon to entropy ratio will not have suppression factors since the theory has only one scale, the string scale or the Planck scale. Hence, we expect the observed value is obtained in these scenarios.

In subsection 4.2 we present a model and show how it satisfies the three conditions for baryogenesis. In subsection 4.3 we calculate the resultant lepton asymmetry by considering Boltzmann equations and show that these scenarios can explain the observed baryon asymmetry. In subsection 4.4 we give some comments.

4.2 A model

In this subsection we present a model of string-scale baryogenesis. Here we consider the following case: the nature is described by the MSM below the string scale. There is not SUSY, nor GUT, nor inflation. Indeed, non-SUSY, non-GUT string models have been proposed [73].

Hence, as an effective theory of string theory, we consider a model whose matter content is the same as that of the MSM. For simplicity, we consider lower-dimensional operators. Let us consider the model,

$$\begin{aligned}
\mathcal{L} = & \mathcal{L}_{\text{MSM}} \\
& + \frac{1}{4} \frac{g_{st}^2}{m_{st}} h_{ij} \epsilon^{\alpha\beta} (\epsilon_{ab} \epsilon_{cd} + \epsilon_{ad} \epsilon_{cb}) l_{\alpha}^{ia} \phi^b l_{\beta}^{jc} \phi^d + \text{h.c.} \\
& + \frac{1}{4} \frac{g_{st}^2}{m_{st}^2} \epsilon^{\alpha\beta} \epsilon^{\gamma\delta} [C_{ijkl} (\delta_{ac} \delta_{bd} + \delta_{ad} \delta_{bc}) + C'_{ijkl} (\delta_{ac} \delta_{bd} - \delta_{ad} \delta_{bc}) + C''_{ijkl} \epsilon_{ab} \epsilon_{cd}]
\end{aligned}$$

$$\times l_{\alpha}^{ia} l_{\beta}^{jb} l_{\gamma}^{kc*} l_{\delta}^{ld*}, \quad (4.43)$$

where l 's are the lepton doublets and ϕ is the Higgs doublet. The string coupling constant and the string scale are g_{st} and m_{st} , respectively. Also, i, j, k and l are generational indices, α, β, γ and δ are spinorial indices, and a, b, c and d are $SU(2)_L$ gauge-group indices.

The first term violates lepton number conservation since it is a Majorana-type coupling. The second term is included to incorporate CP violation. Through a unitary transformation, the coefficient of the first term, h_{ij} , can be rotated into a real diagonal form. However, if the second term is present we cannot guarantee that both terms can be rotated to real forms simultaneously. With two or more generations, this model violates CP invariance. Henceforth, we consider exactly two generations for simplicity .

In the remainder of this subsection we speculate on the departure from thermal equilibrium. First of all, let us consider how the universe would have been in the context of string theory if thermal equilibrium had been maintained [71, 72]. Since the density of states is exponentially increasing in string theory, it has a limiting temperature, the Hagedorn temperature,

$$T_{\text{H}} = \begin{cases} m_{\text{st}}/2\sqrt{2}\pi \sim 5.93 \times 10^{16} \text{ GeV}, & (\text{type II}) \\ m_{\text{st}}/(2 + \sqrt{2})\pi \sim 4.92 \times 10^{16} \text{ GeV}. & (\text{heterotic string}) \end{cases} \quad (4.44)$$

While the universe is contracting, the energy density increases but the temperature remains just below the Hagedorn temperature. When the energy density is low compared to the string scale, matter is composed of particles, or the excitations of short strings whose lengths are of the order of m_{st}^{-1} . However, the high-energy limit of the single-string density of states is found to be [72]

$$\omega(\epsilon) = \frac{\exp(\epsilon/T_{\text{H}})}{\epsilon}. \quad (4.45)$$

When we consider the microcanonical ensemble, it turns out that long strings traverse the entire volume of the universe in a sufficiently high energy density.

Next we consider whether thermal equilibrium is actually realized, by comparing the rates for the thermalization processes with the expansion rate of the universe, the Hubble rate. When matter is composed of particles, the rates for thermalization processes are $\Gamma_{\text{th}} \sim g_* \alpha_{\text{st}}^2 T$, and the Hubble expansion rate is $H = 1.66 g_*^{1/2} T^2 / m_{\text{pl}}$, where m_{pl} and g_* are the Planck mass and the number of matter species, respectively, and $\alpha_{\text{st}} = g_{\text{st}}^2 / 4\pi$. Hence, above the temperature $T_{\text{eq}} \sim g_*^{1/2} \alpha_{\text{st}}^2 m_{\text{pl}} / 1.66 \sim 3.8 \times 10^{16} \text{ GeV}$, or above the energy density $\rho_{\text{eq}} \sim (1.6 \times 10^{17} \text{ GeV})^4$, the thermalization processes are too slow to maintain equilibrium

distributions. However, in the long-string phase, the rates for thermalization processes are proportional to the densities of the string-bits, E/V , where E and V are the total energy and the volume of the universe, respectively. Since the Hubble expansion rate is proportional to the square root of the energy density, $\sqrt{E/V}$, the rates for thermalization processes will dominate the Hubble rate for sufficiently high energy density. Therefore, there will be a critical energy density ρ_* , above which equilibrium distributions are realized.¹¹ Below ρ_* , interactions freeze out and matter distributions are merely affected by the expansion of the universe and depart from thermal equilibrium distributions.

Decay processes of higher excited states begin when the energy density decreases to $\rho_{\text{decay}} \sim (3.7 \times 10^{17} \text{ GeV})^4$, where the decay rates $\sim \alpha_{\text{st}} m_{\text{st}}$ dominate the Hubble expansion rate. These processes are not adiabatic since the matter distributions have departed from equilibrium ones.

During the decay processes of higher excited states, baryon asymmetry as well as entropy is generated. We can make a rough estimate,

$$n_B/s \sim \alpha_{\text{st}}^2 \sim 10^{-3}, \quad (4.46)$$

since the first nontrivial contribution to CP violation comes from the interference of the lowest-order diagrams and the one-loop corrections.

However, if many processes occur at $\rho = \rho_{\text{decay}}$, some cancellations among the decay processes can decrease the above result. These cancellations might be possible if many excited states are taken into account, since ten-dimensional superstring theory has no CP violation originally. The cancellations might be explained also since CPT invariance and unitarity assure the relation $\sum_X \Gamma(X \rightarrow b) = \sum_X \Gamma(X \rightarrow \bar{b})$.

We cannot make a precise estimate since we do not know the dynamics of the decay processes in detail. Hence let us consider the following case: baryon asymmetry is generated after the decay, while it is not generated during the decay due to exact cancellations. By considering this case, we can give a lower bound on n_B/s . We assume that the following matter distributions are caused by the decay processes:

$$n_\phi = n_{\phi^*} \neq n_l = n_{l^*}, \quad (T = T_H) \quad (4.47)$$

where n_ϕ and n_l are the number densities of the Higgs bosons and lepton doublets, respectively. These nonequilibrium distributions are maintained until the temperature of the

¹¹ Thus the initial condition $n_B = n_L = 0$ is assured for sufficiently high energy density.

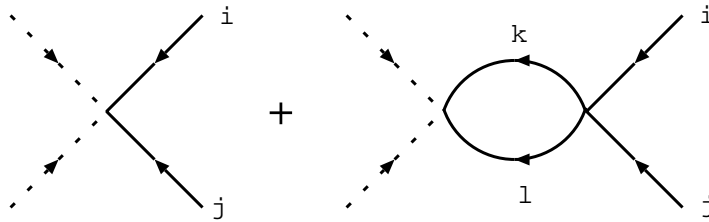


Figure 3: Diagrams which contribute to leptogenesis. The first nontrivial contributions come from the interference between tree-level amplitudes and one-loop corrections. The indices i, j, k and l represent the generations.

universe decreases to T_{eq} . During this epoch a lepton asymmetry is generated. This lepton asymmetry will be converted into a baryon asymmetry of the same order of magnitude *via* sphaleron processes. In the next subsection, we estimate the resultant lepton asymmetry by using the nonequilibrium distribution of Eq.(4.47) as an initial condition.

Finally, we make a brief comment on another scenario which causes nonequilibrium distributions. If we assume the inflationary universe, inflaton decay processes cause nonequilibrium. While the inflaton decays, a baryon asymmetry as well as entropy can be generated [74]. Even if a baryon asymmetry is not generated during the decay processes, some nonequilibrium distributions like those of Eq.(4.47) are generated. Then a baryon asymmetry is generated after the inflaton decays.

4.3 Boltzmann equations

In this subsection we calculate the resultant lepton asymmetry by using the model of Eq.(4.43) and the nonequilibrium distributions of Eq.(4.47). We consider the processes $ll \leftrightarrow \phi^* \phi^*$ and processes related by CP conjugation. The first nontrivial contributions to the generation of lepton asymmetry come from the interference terms of the tree-level amplitudes and the one-loop corrections shown in Fig. 3. These are proportional to $\Im(\sum_{k,l} h_{ij}^* C_{ijkl} h_{kl}) \Im(I)$, where I is a factor coming from the loop integrations. However, they vanish if we naively sum over the indices for generations i and j , since $C_{ijkl}^* = C_{klji}$, as is evident from the Lagrangian of Eq.(4.43). Hence, we consider the processes shown in Fig. 4 in order to produce a different number density for generation 1 and generation 2.

For simplicity, we make the assumption that the distributions for matter remain near equilibrium, $\rho \sim \exp(\frac{E-\mu}{T})$ and $\mu \ll T$. Thus the Boltzmann equations for the above

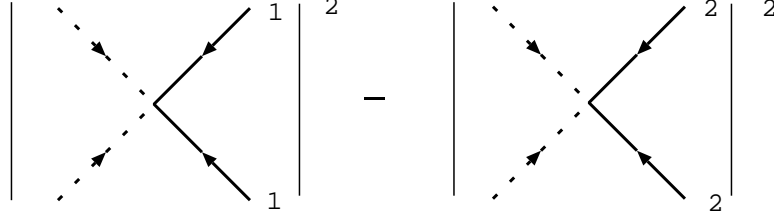


Figure 4: Processes which produce a different number density for generation 1 and generation 2.

processes are as follows:

$$\dot{Y}_l + \Gamma_{\text{th}}(Y_l - 1) = 0, \quad (4.48)$$

$$\dot{Y}_\phi + \Gamma_{\text{th}}(Y_\phi - 1) = 0, \quad (4.48)$$

$$Y_{1-2} + \Gamma_{\text{th}}Y_{1-2} = \frac{3}{\pi} \left(\frac{\alpha_{\text{st}}}{m_{\text{st}}} \right)^2 (h_{11}^2 - h_{22}^2) T^3 (Y_\phi^2 - Y_l^2), \quad (4.49)$$

$$\dot{Y}_L = -\frac{72}{\pi} \frac{\alpha_{\text{st}}^3}{m_{\text{st}}^4} h_{11} h_{22} \Im(C_{1122}) T^5 (Y_{l_1}^2 - Y_{l_2}^2), \quad (4.50)$$

where $Y_i = n_i/n^{(\text{eq})}$. $Y_{1-2} = Y_{l_1} - Y_{l_2}$, $Y_L = Y_{l_1} + Y_{l_2} - (Y_{l_1^*} + Y_{l_2^*})$. Here $\Gamma_{\text{th}} \approx g_* \alpha_{\text{st}}^2 T$ is the rate for thermalization. We use the convention here in which the coefficient of the Majorana-type interactions, h_{ij} , is in real diagonal form.

Equations (4.48) represent the thermalization processes which reduce the nonequilibrium distributions of Eq.(4.47) imposed as an initial condition to the equilibrium distributions. Equation (4.49) represents the processes which produce the difference in the number densities between the generations. Finally, the third equation, Eq.(4.50), represents the production of a lepton asymmetry. The right-hand sides of Eqs. (4.49) and (4.50) are given by calculating the amplitudes shown in Fig. 4 and Fig. 3, respectively, and performing the phase space integrations.

The Boltzmann equations are integrated to give

$$Y_L = -\frac{36}{\pi^2} \alpha_{\text{st}}^5 \left(\frac{m_{\text{pl}}}{1.66 g_*^{1/2} m_{\text{st}}} \right)^2 \left(\frac{T_{\text{H}}}{m_{\text{st}}} \right)^4 J \quad (4.51)$$

$$\approx 2.7 \times 10^{-12} J, \quad (4.52)$$

where

$$J = (h_{11}^2 - h_{22}^2) h_{11} h_{22} \Im(C_{1122}) K, \quad (4.53)$$

$$\begin{aligned}
K &= 12(T_{\text{eq}}/T_{\text{H}})^4 \int_{T_{\text{eq}}/T_{\text{H}}}^{\infty} dz z^{-4} (\exp(-z) + A_l \exp(-2z)) \\
&\quad \times \int_{T_{\text{eq}}/T_{\text{H}}}^z dz' z'^{-2} (2(A_{\phi} - A_l) + (A_{\phi}^2 - A_l^2) \exp(-z')) \quad (4.54)
\end{aligned}$$

$$\begin{aligned}
&\approx 0.538(A_{\phi} - A_l) + 0.173A_l(A_{\phi} - A_l) \\
&\quad + 0.108(A_{\phi}^2 - A_l^2) + 0.0355A_l(A_{\phi}^2 - A_l^2), \quad (4.55)
\end{aligned}$$

$$A_i = (Y_i(T_{\text{H}}) - 1) \exp(T_{\text{eq}}/T_{\text{H}}), \quad (4.56)$$

and $T_{\text{eq}} = g_*^{1/2} \alpha_{\text{st}}^2 m_{\text{pl}} / 1.66 \sim 3.75 \times 10^{16}$ GeV is the temperature below which thermalization processes begin. In the estimations of Eqs. (4.52) and (4.55) we used the following values: $\alpha_{\text{st}} = 1/45$, $g_* = 106.75$, $m_{\text{pl}} = 1.22 \times 10^{19}$ GeV, $m_{\text{st}} = 5.27 \times 10^{17}$ GeV and $T_{\text{H}} = 4.92 \times 10^{16}$ GeV.

The lepton-to-entropy ratio is

$$n_L/s \approx Y_L/g_* \approx 2.6 \times 10^{-14} J, \quad (4.57)$$

where J is given by Eq.(4.53) and its value can be a few thousand if h_{ij} and C_{ijkl} are about five. This lepton asymmetry will be converted into baryon asymmetry of the same order of magnitude *via* sphaleron processes. Therefore, the observed baryon asymmetry can be generated after the decay processes of higher excited states of string theory.

If we take into account the baryogenesis during the decay processes, we will obtain a larger value for the baryon-to-entropy ratio. Too large a value could be diluted afterwards by considering entropy generation in the confinement-deconfinement phase transition, for example. Therefore, the observed baryon-to-entropy ratio can be explained in these scenarios.

4.4 Some comments

We make some comments on the model of Eq.(4.43). We have considered Majorana-type interactions plus four-fermion interactions other than the MSM in order to introduce CP violation. It seems that only Majorana-type interactions would be sufficient since there are Yukawa couplings in the MSM already. The Yukawa plus Majorana-type interactions,

$$y_{ij} e^{*i\alpha} l_{\alpha}^{aj} \phi_a^* + \frac{1}{4} \frac{g_{\text{st}}^2}{m_{\text{st}}} h_{ij} \epsilon^{\alpha\beta} (\epsilon_{ab} \epsilon_{cd} + \epsilon_{ad} \epsilon_{cb}) l_{\alpha}^{ia} \phi^b l_{\beta}^{jc} \phi^d + \text{h.c.}, \quad (4.58)$$

would also work, since, after the Yukawa coupling is brought to the form of a real diagonal matrix *via* a unitary transformation, no degrees of freedom remain to insure a real

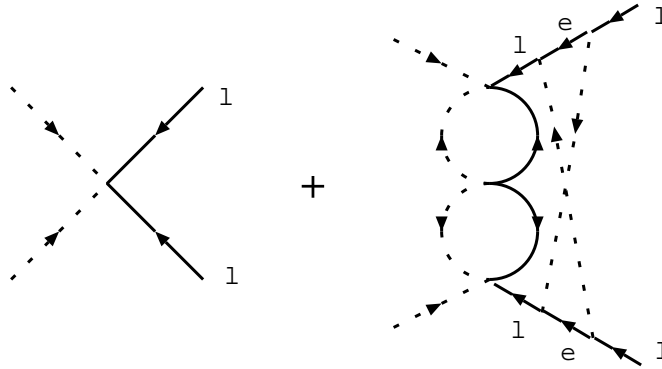


Figure 5: Diagrams which contribute to leptogenesis by means of Yukawa couplings and Majorana-type couplings. The left-handed lepton doublets and the right-handed lepton singlets are l and e , respectively.

Majorana-type coupling. However, because the Yukawa coupling is small, the resultant lepton asymmetry is too small to explain the observed value of n_B/s . Indeed, a lepton asymmetry is generated, for example, through the processes shown in Fig. 5. The result is of the following order:

$$\begin{aligned}
 n_L/s &\sim \left(h \frac{\alpha_{\text{st}}}{m_{\text{st}}}\right)^4 y^4 \frac{m_{\text{pl}}}{1.66 g_*^{1/2}} T_{\text{H}}^3 \frac{1}{g_*} \\
 &\sim 6.7 h^4 \times 10^{-21}.
 \end{aligned}
 \tag{4.59}$$

Here h and y are characteristic values for h_{ij} and y_{ij} , respectively. We think h is of the order one, and we used the Yukawa coupling of the tau lepton for y .

Finally, the Majorana-type terms in Eq.(4.43) give neutrino masses of the order of¹²

$$m_\nu \sim h \frac{g_{\text{st}}^2}{m_{\text{st}}} v^2 \sim 3.2 h \times 10^{-5} \text{ eV}.
 \tag{4.60}$$

This value is consistent with the results of the solar neutrino experiments, if we consider the vacuum oscillation [76] or take into consideration the magnetic field in the sun [77], but it is inconsistent with the results of the atmospheric neutrino experiments.

5 Conclusions and Discussions

In this article, we considered the origins of the observed baryon asymmetry of the universe. Several plausible origins are possible: in the electroweak theory, the grand unified theory,

¹² Similar results are given in [75].

the string theory, *etc.* However, we do not know which origin or which combination of them really explain the observed baryon asymmetry. The origin of the baryon asymmetry has not been established yet.

At the string scale or the Planck scale, the three Sakharov's conditions for baryogenesis are satisfied and the observed baryon asymmetry can be generated, as we saw in section 4. In order to calculate the precise value, we must understand the dynamics of string theory in more detail.

If the baryon asymmetry generated at high temperature vanishes due to washing out by some baryon number violating interactions in thermal equilibrium, or/and dilution by entropy generation in phase transition, or/and dilution by inflation of the universe, *etc.* it must be generated again at lower temperatures. For the baryogenesis at the GUT scale and below, we can use field theory so that more precise estimates are possible.

Within the minimal standard model of the electroweak interactions, it is difficult to explain the observed baryon asymmetry, due to the insufficient electroweak phase transition and the too small CP violation. Hence some extensions are necessary. Until now, many extended models have been studied and shown to generate the observed baryon asymmetry at the electroweak scale. Hence we cannot specify the model beyond the MSM now. However, further progress in the understanding of the Higgs sector and CP violation is expected from the near-future experiments: high energy collider experiments, B-meson experiments, measurements of electric dipole moments of neutron and atoms, *etc.* It will help to establish or rule out the electroweak origin of the baryon asymmetry.

Acknowledgements

I would like to thank K. Hagiwara, who organized the KEK meeting. I would like to thank K. Funakubo, K. Inoue, H. Kawai, Y. Okada and A. Sugamoto for useful discussions. I am also grateful to Z. Fodor for carefully reading the manuscript.

References

- [1] For reviews, see: E. W. Kolb and M. S. Turner, *Ann. Rev. Nucl. Part. Sci.* **33** (1983) 645;
E. W. Kolb and M. S. Turner, *The Early Universe*, (Addison Wesley, California, 1990).
- [2] V. A. Kuzumin, V. A. Rubakov, M. E. Shaposhnikov, *Phys. Lett.* **B155** (1985) 36.
- [3] For reviews, see: A. G. Cohen, D. B. Kaplan and A. E. Nelson, *Ann. Rev. Nucl. Part. Sci.* **43** (1993) 27;
K. Funakubo, *Prog. Theor. Phys.* **96** (1996) 475.
- [4] V. A. Rubakov and M. E. Shaposhnikov, *Usp. Fiz. Nauk* **166** (1996) 493, hep-ph/9603208.
- [5] M. Yoshimura, *Phys. Rev. Lett.* **41** (1978) 281;
S. Weinberg, *Phys. Rev. Lett.* **42** (1979) 850.
- [6] H. Aoki and H. Kawai, KEK-TH-515, hep-ph/9703421.
- [7] I. Affleck and M. Dine, *Nucl. Phys.* **B249** (1985) 361;
M. Dine, L. Randall and S. Thomas, *Nucl. Phys.* **B458** (1996) 291.
- [8] R. Brandenberger, A.-C. Davis, T. Prokopec and M. Trodden, *Phys. Rev.* **D53** (1996) 4257.
- [9] A. G. Cohen, A. De Rújula and S. L. Glashow, BUHEP-97-19, astro-ph/9707087.
- [10] Review of Particle Physics, *Phys. Rev.* **D 54**(1996) 109.
- [11] A. D. Sakharov, *JETP Lett.* **5** (1967) 24.
- [12] G. 't Hooft, *Phys. Rev. Lett.* **37** (1976) 8; **14** (1976) 3432; *Phys. Rev.* **D18** (1978) 2199.
- [13] N. S. Manton, *Phys. Rev.* **D28** (1983) 2019;
F. R. Klinkhamer and N. S. Manton, *Phys. Rev.* **D30** (1984) 2212.
- [14] N. H. Christ, *Phys. Rev.* **D21** (1980) 1591
- [15] A. A. Belavin, A. M. Polyakov, A. S. Schwartz, S. Tyupkin, *Phys. Lett.* **B59** (1975) 85.

- [16] A. Ringwald, Nucl. Phys. **B330** (1990) 1.
- [17] O. Espinosa, Nucl. Phys. **B343** (1990) 310.
- [18] I. Affleck, Nucl. Phys. **B191** (1981) 429.
- [19] T. Harano, M. Sato, KUNS-1391, hep-ph/9703457;
For a review, see: H. Aoyama, T. Harano, H. Kikuhci, I. Okouhci, M. Sato and S. Wada, KUCP-0104, hep-th/9704025.
- [20] M. Mattis, Phys. Rep. **214** (1992) 159.
- [21] V. V. Khoze, A. V. Ringwald, Phys. Lett. **B259** (1991) 106.
- [22] H. Aoki, Prog. Theor. Phys. **91** (1994) 171.
- [23] R. Guida, K. Konishi, N. Magnoli, Int. J. Mod. Phys. **A9** (1994) 795.
- [24] S. Yu. Klebnikov, V. A. Rnbakov, R. G. Tinyakov, Nucl. Phys. **B367** (1991) 334
- [25] T. M. Gould, S. D. H. Hsu. and E. R. Poppitz, Nucl. Phys. **B437** (1995) 83.
- [26] J. S. Langer, Ann. of Phys. **41** (1967) 108; **54** (1969) 258.
- [27] I. Affleck, Phys. Rev. Lett. **46** (1981) 388.
- [28] P. Arnold and L. McLerran, Phys. Rev. **D36** (1987) 581.
- [29] L. Carson, X. Li, L. McLerran, R. Wang, Phys. Rev. **D42** (1990) 2127.
- [30] J. Ambjørn and A. Krasnitz, Phys. Lett. **B362** (1995) 97.
- [31] P. Arnold, D. Son and L. G. Yaffe, Phys. Rev. **D55** (1997) 6264.
- [32] M. Fukugita and T. Yanagida, Phys. Rev. **D42** (1990) 1285.
- [33] J. A. Harvey and M. S. Turner, Phys. Rev. **D42** (1990) 3344.
- [34] H. Georgi and S. L. Glashow, Phys. Rev. Lett. **32** (1974) 438.
- [35] J. M. Cline, K. Kainulainen and K. A. Olive, Phys. Rev. **D49** (1994) 6394.
- [36] M. E. Shaposhnikov, JETP Lett. **44** (1986) 465; Nucl. Phys. **B287** (1987) 757.

- [37] M. Joyce, T. Prokopec, N. Turok, Phys. Rev. **D53** (1996) 2930; **D53** (1996) 2958.
- [38] A. G. Cohen, D. B. Kaplan and A. E. Nelson, Phys. Lett. **B263** (1991) 86.
- [39] A. E. Nelson, D. B. Kaplan and A. G. Cohen, Nucl. Phys. **B373** (1992) 453.
- [40] M. Dine, R. L. Leigh, P. Huet, L. Linde, D. Linde, Phys. Lett. **B283** (1992) 319; Phys. Rev. **D46** (1992) 550.
- [41] K. Funakubo, A. Kakuto, S. Otsuki, F. Toyoda, SAGA-HE-121, hep-ph/9704359.
- [42] K. Funakubo, A. Kakuto, S. Otsuki, F. Toyoda, Prog. Theor. Phys. **95** (1996) 929.
- [43] M. Dine and S. Thomas, Phys. Lett. **B328** (1994) 73.
- [44] A. G. Cohen, D. B. Kaplan and A. E. Nelson, Phys. Lett. **B336** (1994) 41
- [45] M. Kobayashi, T. Maskawa, Prog. Theor. Phys. **49** (1973) 652.
- [46] C. Jarlskog, Phys. Rev. Lett. **55** (1985) 1039.
- [47] G. R. Farrar and M. E. Shaposhnikov, Phys. Rev. Lett. **70** (1993) 2833; **71** (1993) 210; Phys. Rev. **D50** (1994) 774.
- [48] M. B. Gavela, P. Hernandez, J. Orloff, O. Pène and C. Quimbay, Mod. Phys. Lett. **9** (1994) 795; Nucl. Phys. **B430** (1994) 382; P. Huet and E. Sather, Phys. Rev. **D51** (1995) 379.
- [49] L. Dolan, R. Jackiw, Phys. Rev. **D9** (1974) 3320.
- [50] P. Arnold and O. Espinosa, Phys. Rev. **D47** (1993) 3546.
- [51] Z. Fodor and A. Hebecker, Nucl. Phys. **B432** (1994) 127.
- [52] B. Bunk, E.-M. Ilgenfritz, J. Kripfganz and A. Shiller, Phys. Lett. **B284** (1992) 371; Nucl. Phys. **B403** (1993) 453.
- [53] Z. Fodor, J. Hein, K. Jansen, A. Jaster, I. Montvay and F. Csikor, Phys. Lett. **B334** (1994) 405; Z. Fodor, J. Hein, K. Jansen, A. Jaster and I. Montvay, Nucl. Phys. **B439** (1995) 147; F. Csikor, Z. Fodor, J. Hein, A. Jaster and I. Montvay, Nucl. Phys. **B474** (1996) 421.

- [54] Y. Aoki, UTCCP-P-20, hep/lat/9612023.
- [55] K. Kajantie, K. Rummukainen and M. Shaposhnikov, Nucl. Phys. **B407** (1993) 356;
K. Farakos, K. Kajantie, K. Rummukainen and M. Shaposhnikov, Phys. Lett. **B336**
(1994) 494;
K. Kajantie, M. Laine, K. Rummukainen and M. Shaposhnikov, Nucl. Phys. **B466**
(1996) 189;
K. Kajantie, M. Laine, K. Rummukainen and M. Shaposhnikov, Phys. Rev. Lett. **77**
(1996) 2887.
- [56] E.-M. Ilgenfritz, J. Kripfganz, H. Perlt and A. Shiller, Phys. Lett. **B356** (1995) 561;
M. Gürtler, E.-M. Ilgenfritz, J. Kripfganz, H. Perlt and A. Shiller, Nucl. Phys. **B483**
(1997) 383.
- [57] For a review, see: S.M. Barr, Int. J. Mod. Phys.**A8** (1993) 209.
- [58] N. Turok and J. Zadrozny, Nucl. Phys. **B369** (1992) 729.
- [59] A. Brignol, J. R. Espinosa, M. Quirós and F. Zwirner, Phys. Lett. **B324** (1994) 181;
M. Carena, M. Quirós and C. E. M. Wagner, Phys. Lett. **B380** (1996) 81.
- [60] D. Delepine, J.-M. Gérard, R. Gonzalez Felipe and J. Weyers, Phys. Lett. **B386** (1996)
183.
- [61] J. R. Espinosa, Nucl. Phys. **B475** (1996) 273.
- [62] P. Huet and A. E. Nelson, Phys. Rev. **D53** (1996) 4578.
- [63] M. Aoki, N. Oshimo and A. Sugamoto, OCHA-PP-87, hep-ph/9612225; OCHA-PP-96,
hep-ph/9706287.
- [64] M. Carena, M. Quirós, A. Riotto, I. Vilja and C. E. M. Wagner, CERN-TH/96-242,
hep-ph/9702409;
M. Carena and C. E. M. Wagner, CERN-TH/97-74, hep-ph/9704347.
- [65] W. Fischler, S. Paban and S. Thomas, Phys. Lett. **B289** (1992) 373.
- [66] Y. Kizukuri and N. Oshimo, Phys. Rev. **D46** (1992) 3025.
- [67] M. P. Worah, SLAC-PUB-7417, hep-ph/9702423; SLAC-PUB-7476, hep-ph/9704389.

- [68] A. Yamaguchi and A. Sugamoto, *Mod. Phys. Lett.* **A9**(1994) 2599.
- [69] T. Uesugi, A. Sugamoto and A. Yamaguchi, *Phys. Lett.* **B392** (1997) 389.
- [70] J. McDonald, *Phys. Rev.* **D53** (1996) 645.
- [71] R. Hagedorn, *Nuovo Cim. Suppl.* **3** (1965) 147;
K. Huang and S. Weinberg, *Phys. Rev. Lett.* **25** (1970) 895;
J. J. Atick and E. Witten, *Nucl. Phys.* **B310** (1988) 219.
- [72] R. Brandenberger and C. Vafa, *Nucl. Phys.* **B316** (1989) 391;
D. A. Lowe and L. Thorlacius, *Phys. Rev.* **D51** (1995) 665.
- [73] For a review, see: K. R. Dienes, IASSNS-HEP-95-97, hep-th/9602045.
- [74] A. D. Dolgov and A. D. Linde, *Phys. Lett.* **116B** (1982) 329;
L. F. Abbott, E. Farhi and M. B. Wise, *Phys. Lett.* **117B** (1982) 29.
- [75] M. Fukugita and A. Suzuki (Eds.), *Physics and Astrophysics of Neutrinos*, (Springer-Verlag, Tokyo, 1994).
- [76] N. Hata and P. Langacker, IASSNS-AST 97/29, hep-ph/9705339.
- [77] T. Kubota, T. Kurimoto and E. Takasugi, *Phys. Rev.* **D49** (1994) 2462.